



Journal of Applied and Computational Mechanics



Research Article

An Analysis of Thermal-Bending Stresses in a Simply Supported Thin Elliptical Plate

Vinod Varghese

Department of Mathematics, Smt. Sushilabai Rajkamalji Bharti Science College
Arni, Yavatmal, India, vino7997@gmail.com,

Received December 10 2017; Revised January 17 2018; Accepted for publication January 27 2018.
Corresponding author: Vinod Varghese, vino7997@gmail.com,
Copyright © 2018 Shahid Chamran University of Ahvaz. All rights reserved.

Abstract. In this paper, a transient thermal stress investigation on a simply supported thin elliptical plate during sectional heating with time-dependent temperature supply is considered. The solution of heat conduction equation with corresponding initial and boundary conditions is obtained by employing an integral transform approach. The governing equation solution for the small deflection theory is obtained and utilized to preserve the intensities of thermal bending moments, involving the Mathieu and modified functions and its derivatives. The deflection results show an approximately good agreement with the previously given results. It is also demonstrated that the temperature field in a circular solution could be resulted in a particular case of the present mathematical solution. The obtained numerical results utilizing computational implements are precise enough for practical purposes.

Keywords: Elliptical solid plate, Temperature distribution, Thermal stresses, Elliptical coordinate, Integral transform, Mathieu function.

1. Introduction

The determination of thermal stresses using bending moments, twisting moments, and shearing forces in thin plate structures conventionally experienced difficulties during the analysis phase and for design purposes. Consequently, few theoretical studies concerning them have been reported so far. For example, Jane and Hong [1] investigated interlaminar stresses and displacements in a simply supported thin laminated rectangular orthotropic plate with four-sided edges under bending using the generalized differential quadrature (GDQ) technique. Mathews and Shabna [2] studied the static and thermal analysis of isotropic rectangular plates composed of different materials with and without cut-outs having different boundary conditions by varying the aspect ratio utilizing numericals as well as by the finite element method. Deshmukh et al. [3] obtained the thermal stress components in a thin simply supported rectangular plate due to the thermal bending and the shearing stress function utilizing integral transform methods. Cheng and Fan [4] analyzed the thin rectangular plate with one simply supported edge while other edges are set free under the temperature disparity predicated on the small deflection theory and the superposition principle by considering the temperature variation that is perpendicular to the surface. Few authors [5, 6] have obtained a small deflection based on the small deflection theory. A short history of the research work associated with the small deflection and bending stresses insights various approximate methods like the Ritz energy method, Galerkin's Method, finite element models and perturbation theory to solve the system. The most highly cited literature review on thin plates and shells theory was directed by Ventsel and Krauthammer [7] in their book. So far, many research have been carried out on the mechanical and thermomechanical behaviour of simply supported different geometrical profiles while very few work is available on the elliptical structure. This might be due to the mathematical complications and that closed-form solutions for heat conduction problems in an elliptical object are rare in literature though the studies are very extensive. These elliptical



plates or cylinders are widely used as structural elements in various applications due to their elementary geometry. During literature review, only a few reports were observed which extensively studied with elliptical objects. For example, Laura and Rossit [8] considered the exact analytical solution of thermal bending of clamped, anisotropic, and elliptic plates in the case where the thermal field is given by an expression of the type $T(x,y,z)=z(Ax^2+Cxy+By^2)$. Sato [9] proposed the purely analytical solution predicated on the classical small-deflection theory for deflection due to the bending of a clamped elliptical plate subjected to the combined action of uniform lateral load distributed over its entire surface and uniform in-plane force distributed at its middle plane derived in the elliptical cylinder coordinate system. Very recently, Bhad et al. [10-12] and Dhakate et al. [13] determined the thermal bending moments, involving the Mathieu functions and modified functions along with its derivatives over a thin elliptical object utilizing few new integral transform methods. Though, it has been substantiated that ample cases of thermoelastic bending stresses in solids have led to various technical problems in mechanical applications on which the produced heat is rapidly sought to be transferred or dissipated. The primary purpose of the current study is to take advantage of a new integral transform technique using Mathieu functions and modified Mathieu functions of order n to fill this consequential gap and obtain the exact solution. This paper proposes an operational method to determine more general closed-form solutions by establishing a new integral transform in the elliptical coordinate. The paramountcy of proposed transform over the previously published techniques [14] can be seen while obtaining the temperature of any height for elliptical object profile. The theoretical calculations are studied using the dimensional parameter whereas graphical calculations are carried out using the dimensionless parameter. The prosperity of this research mainly lies on the incipient mathematical procedures which present a much more straightforward approach for optimization of the design in regard to material usage and performance in engineering problems and concretely in the determination of thermoelastic deformation in the annular sector plate used as the foundation of pressure vessels, furnaces, etc.

2. Formulation of the problem

Considering a thin elliptical solid plate occupying the space $D = \{(\xi, \eta, z) \in R^3 : 0 < \xi < \xi_0, 0 < \eta < 2\pi, 0 \leq z \leq \ell\}$, defined by the transformation $\xi + i\eta = \cosh^{-1}[(x + iy)/c]$, $z = z$, and length $2c$ is the distance between their prevalent foci which can be defined as $2c = 2(a^2 - b^2)^{1/2}$, explicitly, the following relation is obtained:

$$x = c \cosh \xi \cos \eta, y = c \sinh \xi \sin \eta, z = z \tag{1}$$

and the scale factor is

$$h^2 = 2/[c^2 (\cosh 2\xi - \cos 2\eta)] \tag{2}$$

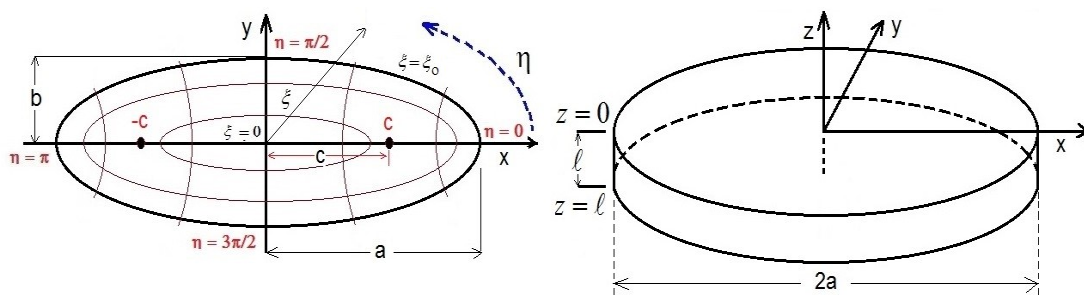


Fig. 1. Elliptical plate configuration

The curves $\eta = constants$ represent a family of confocal hyperbolas while the curves $\xi = constants$ represent a family of confocal ellipses. Therefore, both sets of curves intersect each other orthogonally at every point in space. Now, we consider the elliptical plate along the semi-major axis as a whereas semi-minor axis as b . The parameter ξ defines the interfocal lines having the range of $\xi \in (0, \xi_0)$, that can be given as $\xi = \tanh^{-1}(b/a)$ as shown in Fig. 1.

2.1 Temperature distribution analysis

The boundary value problem of heat conduction [10] of a homogeneous isotropic solid is given as

$$h^2 \left(\frac{\partial^2 T}{\partial \xi^2} + \frac{\partial^2 T}{\partial \eta^2} \right) + \frac{\partial^2 T}{\partial z^2} = \frac{1}{\kappa} \frac{\partial T}{\partial t} \tag{3}$$

which is subjected to the conditions for the temperature field as

$$\left. \begin{aligned} T(\xi, \eta, z, 0) = 0, T(\xi_0, \eta, z, t) = 0, \\ T(\xi, \eta, 0, t) = f(\xi, \eta, t), T(\xi, \eta, \ell, t) = 0 \end{aligned} \right\} \tag{4}$$

in which $T = T(\xi, \eta, z, t)$ is the temperature distribution on the thin elliptical plate, $f(\xi, \eta, t)$ denotes the prescribed

surface temperature (i.e. sectional heat supply source) from the curved surface at $z = 0$, $\kappa = \lambda / \rho C$ represents the thermal diffusivity in which λ is the thermal conductivity of the material, ρ is the density, and C is the calorific capacity. The result of the above-mentioned heat conduction gives thermally induced resultant moment and the resultant force [7] of the plate, respectively, which are defined by

$$\left. \begin{aligned} M_T(\xi, \eta, t) &= \alpha E \int_0^\ell z T(\xi, \eta, z, t) dz \\ N_T(\xi, \eta, t) &= \alpha E \int_0^\ell T(\xi, \eta, z, t) dz \end{aligned} \right\} \quad (5)$$

in which α denotes the coefficient of linear thermal expansion and Young’s Modulus of the material of the plate, respectively. In this step, a simply supported thin elliptical solid plate subjected to a thermal load is taken into consideration. The fundamental differential equation for normal deflection $\omega(\xi, \eta, t)$ and the associated boundary conditions [3] in the elliptical coordinate system are given as

$$D \nabla^2 \omega \nabla^2 \omega + \frac{1}{1-\nu} \nabla^2 M_T = 0 \quad (6)$$

with suitable boundary conditions for simply supported conditions as

$$\omega(\xi_0, \eta, 0) = 0, \quad \omega(\xi, \eta, 0) = \frac{\partial \omega(\xi, \eta, t)}{\partial t} \Big|_{t=0} = 0 \quad (7)$$

Since it is assumed that the plate is sufficiently thin, the plane $\xi\eta$, initially normal to the middle or neutral plane ($z = 0$) afore bending, remains straight and normal to the middle surface during the deformation. Therefore, the basic equations of in-plane resultant forces can be taken as

$$N_{\xi\xi} = N_{\eta\eta} = N_{\xi\eta} = 0 \quad (8)$$

Moreover, the resultant bending moments per unit width can be defined as

$$\left. \begin{aligned} M_{\xi\xi} &= -D h^2 \left\{ \left(\frac{\partial^2 \omega}{\partial \xi^2} + \nu \frac{\partial^2 \omega}{\partial \eta^2} \right) - \frac{(1-\nu) \sinh 2\xi}{(\cosh 2\xi - \cos 2\eta)} \frac{\partial \omega}{\partial \xi} + \frac{(1-\nu) \sin 2\eta}{(\cosh 2\xi - \cos 2\eta)} \frac{\partial \omega}{\partial \eta} \right\} - \frac{M_T}{1-\nu} \\ M_{\eta\eta} &= -D h^2 \left\{ \left(\nu \frac{\partial^2 \omega}{\partial \xi^2} + \frac{\partial^2 \omega}{\partial \eta^2} \right) + \frac{(1-\nu) \sinh 2\xi}{(\cosh 2\xi - \cos 2\eta)} \frac{\partial \omega}{\partial \xi} - \frac{(1-\nu) \sin 2\eta}{(\cosh 2\xi - \cos 2\eta)} \frac{\partial \omega}{\partial \eta} \right\} - \frac{M_T}{1-\nu} \\ M_{\xi\eta} &= -D h^2 (1-\nu) \left\{ \frac{\partial \omega}{\partial \xi} \sin 2\eta + \frac{\partial \omega}{\partial \eta} \sinh 2\xi - \frac{\partial^2 \omega}{\partial \xi \partial \eta} (\cosh 2\xi - \cos 2\eta) \right\} \end{aligned} \right\} \quad (9)$$

At the end of the analysis, while analyzing the thermal bending stress problem for the simply supported elliptical plate, we verify that the resultant bending moment per unit width, as mentioned in the first relation of Eq. (9), must satisfy the following relation

$$M_{\xi\xi}(\xi, \eta, t) = 0 \quad \text{for all } t \text{ and } \xi = \xi_0. \quad (10)$$

2.2 Associated bending thermal stresses

The thermal stress components in terms of resultant forces and resultant moments are given as

$$\left. \begin{aligned} \sigma_{\xi\xi} &= \frac{1}{\ell} N_{\xi\xi} + \frac{12z}{\ell^3} M_{\xi\xi} + \frac{1}{1-\nu} \left(\frac{1}{\ell} N_T + \frac{12z}{\ell^3} M_T - \alpha E T \right) \\ \sigma_{\eta\eta} &= \frac{1}{\ell} N_{\eta\eta} + \frac{12z}{\ell^3} M_{\eta\eta} + \frac{1}{1-\nu} \left(\frac{1}{\ell} N_T + \frac{12z}{\ell^3} M_T - \alpha E T \right) \\ \sigma_{\xi\eta} &= \frac{1}{\ell} N_{\xi\eta} - \frac{12z}{\ell^3} M_{\xi\eta} \end{aligned} \right\} \quad (11)$$

The above-mentioned Eqs. (1) to (11) constitute the mathematical formulation of the problem under consideration.

3. Solution to the problem

By taking the finite Fourier Sine transform of Eq. (3) into consideration, we get

$$h^2 \left(\frac{\partial^2 \bar{T}}{\partial \xi^2} + \frac{\partial^2 \bar{T}}{\partial \eta^2} \right) + \alpha_m \bar{f} - \alpha_m^2 \bar{T} = \frac{1}{\kappa} \frac{\partial \bar{T}}{\partial t} \tag{12}$$

with

$$\bar{T}(\xi, \eta, m, 0) = 0, \bar{T}(\xi_o, \eta, m, t) = 0 \tag{13}$$

in which $\alpha_m = m\pi/\ell$ are the roots of $\sin(\alpha_m) = 0$ with kernel $\sqrt{2/\ell} \sin(\alpha_m)$. To solve the differential Eq. (12), the modified integral transform including Mathieu functions as defined by Gupta [14] of order n and m over the variable ξ and η is introduced as

$$\bar{f}(\pm q_{n,m}) = \int_0^{\xi_o} \int_0^{2\pi} f(\xi, \eta) (\cosh 2\xi - \cos 2\eta) S_{n,m}(\xi, \eta, \pm q_{2n,m}) d\xi d\eta \tag{14}$$

in which the kernel can be given as

$$S_{n,m}(\xi, \eta, \pm q_{2n,m}) = Ce_n(\xi, \pm q_{2n,m}) ce_n(\eta, \pm q_{2n,m}) \tag{15}$$

The inversion theorem of Eq. (14) can be defined as

$$f(\xi, \eta) = \sum_{n=0}^{\infty} \sum_{m=1}^{\infty} \bar{f}(\pm q_{2n,m}) S_{n,m}(\xi, \eta, \pm q_{2n,m}) / C_{2n,m} \tag{16}$$

where $q_{n,m}$ are the roots of the transcendental equation $Ce_n(\xi_o, q) = 0$, $q = \lambda c^2 / 4$ and

$$C_{2n,m} = \int_0^{\xi_o} (\cosh 2\xi - \Theta_{2n,m}) Ce_{2n}^2(\xi, \pm q_{2n,m}) d\xi \tag{17}$$

in which $ce_{2n}(\eta, q)$ is a Mathieu function [15], $Ce_{2n}(\xi, q)$ is a modified Mathieu function [15], and

$$\Theta_{2n,m} = \frac{1}{\pi} \int_0^{2\pi} \cos 2\eta ce_{2n}^2(\eta, \pm q_{2n,m}) d\eta = A_0^{(2n)} A_2^{(2n)} + \sum_{r=0}^{\infty} A_{2r}^{(2n)} A_{2r+2}^{(2n)} \tag{18}$$

in these series, A 's are the functions of q . Applying the integral transformation (14) for the variables (ξ, η) , leads to

$$\alpha_m \bar{f} - (\lambda_{2n,m}^2 + \alpha_m^2) \bar{T} = \frac{1}{\kappa} \frac{\partial \bar{T}}{\partial t} \tag{19-a}$$

with

$$\bar{T}(q_{2n,m}, m, 0) = 0 \tag{19-b}$$

in which $\lambda_{2n,m} = 4q_{n,m} / c^2$. The general solution of Eq. (16) using Eq. (17) is a function as

$$\bar{T} = \exp[-(\kappa \lambda_{2n,m}^2 + \alpha_m^2)t] \left\{ \int_0^t \exp[(\kappa \lambda_{2n,m}^2 + \alpha_m^2)\tau] \alpha_m \bar{f} d\tau \right\} \tag{19-c}$$

For the sake of brevity, the following relation is taken into consideration:

$$f(\xi, \eta, t) = Q_0 \exp(-\omega t) \delta(\xi - \xi_1) \delta(\eta - 2\pi) / 2\pi \xi_1, \tag{19-d}$$

in which $\delta(\xi - \xi_1) = 0$ and $\delta(z - \ell_0) = 0$ everywhere $\xi \neq \xi_1, \xi_1 \in [0, \xi_o]$ and $z \neq \ell_0, z \in [0, \ell]$. By applying finite Fourier Sine transform and the new integral transform (14) on Eq. (19), the following relation is obtained:

$$\bar{f} = Q_0 \exp(-\omega t) (\cosh 2\xi_o - 1) S_{n,m}(\xi_1, \eta, \pm q_{2n,m}) \tag{20}$$

Using the inversion theorem of the finite Fourier Sine transform and then integral transform (15), the following solution is obtained:

$$T = \sum_{\ell=1}^{\infty} \sum_{n=0}^{\infty} \sum_{m=1}^{\infty} \bar{T}(q_{2n,m}, \ell, t) \sin(\alpha_m z) S_{n,m}(\xi, \eta, \pm q_{2n,m}) / C_{2n,m} \tag{21}$$

Using the first relation of Eq. (5) and Eq. (21), one obtains

$$M_T = \alpha E \sum_{\ell=1}^{\infty} \sum_{n=0}^{\infty} \sum_{m=1}^{\infty} \bar{T}(q_{2n,m}, \ell, t) [\sin(\alpha_m \ell) - (\alpha_m \ell) \cos(\alpha_m \ell)] \times S_{n,m}(\xi, \eta, \pm q_{2n,m}) / C_{2n,m} \alpha_m^2 \tag{22}$$

Using Eqs. (6) and (22) yields

$$\omega = 3\alpha(1+\nu) \sum_{n=1}^{\infty} \sum_{n=0}^{\infty} \sum_{\ell=1}^{\infty} \bar{T}(q_{2n,m}, \ell, t) [\sin(\alpha_m \ell) - (\alpha_m \ell) \cos(\alpha_m \ell)] \times S_{n,m}(\xi, \eta, \pm q_{2n,m}) / q_{2n,m} C_{2n,m} \alpha_m \ell^3 \tag{23}$$

Using second relation of Eq. (5) and Eq. (21) leads to

$$N_T = \alpha E \sum_{\ell=1}^{\infty} \sum_{n=0}^{\infty} \sum_{m=1}^{\infty} \bar{T}(q_{2n,m}, \ell, t) [1 - \cos(\alpha_m \ell)] \times S_{n,m}(\xi, \eta, \pm q_{2n,m}) / C_{2n,m} \alpha_m \tag{24}$$

Inserting Eqs. (22) - (23) in Eq. (9) results in

$$\begin{aligned} M_{\xi\xi} = & -3(1+\nu)\alpha D h^2 \sum_{m=1}^{\infty} \sum_{n=0}^{\infty} \sum_{\ell=1}^{\infty} \left\langle \bar{T}(q_{2n,m}, \ell, t) \right. \\ & \times [\sin(\alpha_m \ell) - (\alpha_m \ell) \cos(\alpha_m \ell)] \{ [S_{n,m}(\xi, \eta, \pm q_{2n,m})]_{,\xi\xi} \\ & + \nu S_{n,m}(\xi, \eta, \pm q_{2n,m})_{,\eta\eta} \} - [(1-\nu)c^2 h^2 / 2] \sinh 2\xi \\ & \times [\sinh 2\xi S_{n,m}(\xi, \eta, \pm q_{2n,m})_{,\xi} - \sin 2\eta S_{n,m}(\xi, \eta, \pm q_{2n,m})_{,\eta}] \\ & \left. - [(2\ell^3 E) S_{n,m}(\xi, \eta, \pm q_{2n,m}) / (6(1-\nu^2) h^2 D)] \right\} / q_{2n,m} C_{2n,m} \alpha_m^2 \bigg\rangle / \ell^3 \end{aligned} \tag{25}$$

$$\begin{aligned} M_{\eta\eta} = & -3(1+\nu)\alpha D h^2 \sum_{n=1}^{\infty} \sum_{n=0}^{\infty} \sum_{\ell=1}^{\infty} \left\langle \bar{T}(q_{2n,m}, \ell, t) \right. \\ & \times [\sin(\alpha_m \ell) - (\alpha_m \ell) \cos(\alpha_m \ell)] \{ [\nu S_{n,m}(\xi, \eta, \pm q_{2n,m})]_{,\xi\xi} \\ & - S_{n,m}(\xi, \eta, \pm q_{2n,m})_{,\eta\eta} \} + [(1-\nu)c^2 h^2 / 2] \sinh 2\xi \\ & \times [\sinh 2\xi S_{n,m}(\xi, \eta, \pm q_{2n,m})_{,\xi} - \sin 2\eta S_{n,m}(\xi, \eta, \pm q_{2n,m})_{,\eta}] \\ & \left. - [(2\ell^3 E) S_{n,m}(\xi, \eta, \pm q_{2n,m}) / [6(1-\nu^2) h^2 D]] \right\} / q_{2n,m} C_{2n,m} \alpha_m^2 \bigg\rangle / \ell^3 \end{aligned} \tag{26}$$

$$\begin{aligned} M_{\xi\eta} = & -3(1-\nu^2)\alpha D h^2 \sum_{n=1}^{\infty} \sum_{n=0}^{\infty} \sum_{\ell=1}^{\infty} \left\langle \bar{T}(q_{2n,m}, \ell, t) \right. \\ & \times [\sin(\alpha_m \ell) - (\alpha_m \ell) \cos(\alpha_m \ell)] \{ [\sin(2\eta) S_{n,m}(\xi, \eta, \pm q_{2n,m})]_{,\xi} \\ & + \sinh(2\xi) S_{n,m}(\xi, \eta, \pm q_{2n,m})_{,\eta} \} - c^2 h^2 S_{n,m}(\xi, \eta, \pm q_{2n,m})_{,\xi\eta} / 2 \\ & \left. / q_{2n,m} C_{2n,m} \alpha_m^2 \right\rangle / \ell^3 \end{aligned} \tag{27}$$

Inserting Eqs. (8) and (22) - (27) in Eq. (11), we derive stresses as

$$\begin{aligned} \sigma_{\xi\xi} = & \sum_{m=1}^{\infty} \sum_{n=0}^{\infty} \sum_{\ell=1}^{\infty} \bar{T}(q_{2n,m}, \ell, t) \left\langle \{-6^2 z (1+\nu) \alpha D [\sin(\alpha_m \ell) - (\alpha_m \ell) \right. \\ & \times \cos(\alpha_m \ell)] / \ell^3 h \{ [S_{n,m}(\xi, \eta, \pm q_{2n,m})]_{,\xi\xi} + \nu S_{n,m}(\xi, \eta, \pm q_{2n,m})_{,\eta\eta} \} \\ & - [(1-\nu)c^2 h^2 \sinh(2\xi)] [\sinh(2\xi) S_{n,m}(\xi, \eta, \pm q_{2n,m})_{,\xi} - \sin(2\eta) \\ & \times S_{n,m}(\xi, \eta, \pm q_{2n,m})_{,\eta}] - (\ell^3 E) S_{n,m}(\xi, \eta, \pm q_{2n,m}) / [3(1-\nu^2) h^2 D] \} \\ & + (\alpha_m \alpha E) [(\alpha_m \alpha E) S_{n,m}(\xi, \eta, \pm q_{2n,m}) / (1-\nu)] \{ [1 - \cos(\alpha_m \ell)] / \ell \\ & + 12z [\sin(\alpha_m \ell) - (\alpha_m \ell) \cos(\alpha_m \ell)] / \ell^3 - (\alpha_m) \sin(\alpha_m z) \} \\ & \left. / (1-\nu) \right\rangle / q_{2n,m} C_{2n,m} \beta_m^2 \end{aligned} \tag{28}$$

$$\begin{aligned} \sigma_{\eta\eta} = & \sum_{n=1}^{\infty} \sum_{n=0}^{\infty} \sum_{\ell=1}^{\infty} \bar{T}(q_{2n,m}, \ell, t) \left\langle \{-6^2 z (1+\nu) \alpha D [\sin(\alpha_m \ell) \right. \\ & - (\alpha_m \ell) \cos(\alpha_m \ell)] / \ell^3 h \{ [\nu S_{n,m}(\xi, \eta, \pm q_{2n,m})]_{,\xi\xi} - S_{n,m}(\xi, \eta, \pm q_{2n,m})_{,\eta\eta} \} \\ & + (1-\nu)c^2 h^2 \sinh 2\xi [\sinh 2\xi S_{n,m}(\xi, \eta, \pm q_{2n,m})_{,\xi} \\ & - \sin 2\eta S_{n,m}(\xi, \eta, \pm q_{2n,m})_{,\eta}] / 2 \\ & - (\ell^3 E) S_{n,m}(\xi, \eta, \pm q_{2n,m}) / [3(1-\nu^2) c^2 h^2 D] \} \\ & + [(\alpha_m \alpha E) S_{n,m}(\xi, \eta, \pm q_{2n,m}) / (1-\nu)] \\ & \times \{ [1 - \cos(\alpha_m \ell)] / \ell + 12z [\sin(\alpha_m \ell) - (\alpha_m \ell) \cos(\alpha_m \ell)] / \ell^3 \\ & - (\alpha_m) \sin(\alpha_m z) \} \bigg\rangle / q_{2n,m} C_{2n,m} \alpha_m^2 \end{aligned} \tag{29}$$

$$\begin{aligned} \sigma_{\xi\eta} = & 6^2 z \alpha D (1-\nu^2) \sum_{n=1}^{\infty} \sum_{m=0}^{\infty} \sum_{\ell=1}^{\infty} \bar{T}(q_{2n,m}, \ell, t) \{ [\sin(\alpha_m \ell) \\ & - (\alpha_m \ell) \cos(\alpha_m \ell)] \{ [\sin(2\eta) S_{n,m}(\xi, \eta, \pm q_{2n,m})_{,\xi} + \sinh(2\xi) \\ & \times S_{n,m}(\xi, \eta, \pm q_{2n,m})_{,\eta}] - (c^2 h^2) S_{n,m}(\xi, \eta, \pm q_{2n,m})_{,\xi\eta} / 2 \} \\ & / q_{2n,m} C_{2n,m} \alpha_m^2 \} / h \ell^3 \end{aligned} \tag{30}$$

4. Numerical results, discussion, and remarks

For the sake of simplicity of calculation, we introduce the following dimensionless values:

$$\left. \begin{aligned} \xi_o &= \xi_o / \xi_o, \bar{\xi} = \xi / \xi_o, \bar{z} = z / \xi_o, e = c / \xi_o, \bar{h}^2 = h^2 \xi_o^2, \\ \tau &= \kappa t / \xi_o^2, \bar{T} = T / T_o, \bar{\omega} = \omega / \alpha T_o \xi_o, \\ \bar{\sigma}_{ij} &= \sigma_{ij} / E \alpha T_o, \bar{N}_{ij} = N_{ij} / E \xi_o^3, \bar{M}_{ij} = M_{ij} / E \xi_o^3 \quad (i, j = \xi, \eta) \end{aligned} \right\} \tag{31}$$

By substituting the value of Eq. (31) in Eqs. (21) - (30), we obtain the expressions for temperature, thermal deflection, and thermal stresses for our numerical discussion, respectively. The numerical computations are carried out for the pure Aluminum elliptical plate with the physical parameter as $\xi_o = 1$ m, $\ell = 0.08$ m, the reference temperature as 150°C , and the thermo-mechanical properties were considered as modulus of elasticity $E = 70$ GPa, Poisson’s ratio $\nu = 0.35$, thermal expansion coefficient $\alpha = 23 \times 10^{-6} / ^\circ\text{C}$, thermal diffusivity $\kappa = 84.18 \times 10^{-6} \text{ m}^2\text{s}^{-1}$, and thermal conductivity $\lambda = 204.2 \text{ Wm}^{-1}\text{K}^{-1}$. The positive and real roots of the transcendental equation $Ce_{2n}(\xi_o, q) = 0$ are $q_{2n,m} = 0.089, 0.406, 0.894, 1.640, 2.532, 3.600, 4.932, 6.324, 8.023, 9.789, 12.032, 14.345, 16.789, 19.486, 22.786, 25.342, 28.603, 32.654, 35.854$ and 39.834 . To examine the influence of heating on the plate, we performed the numerical calculation for all variables and numerical calculations which are illustrated by applying MATHEMATICA software. Moreover, Figs. 2–4 illustrate the numerical results of the dimensionless temperature of the elliptical plate under the thermal boundary condition that is subjected to zero temperature on upper and lower face and sectional heat supply on the upper curved surface.

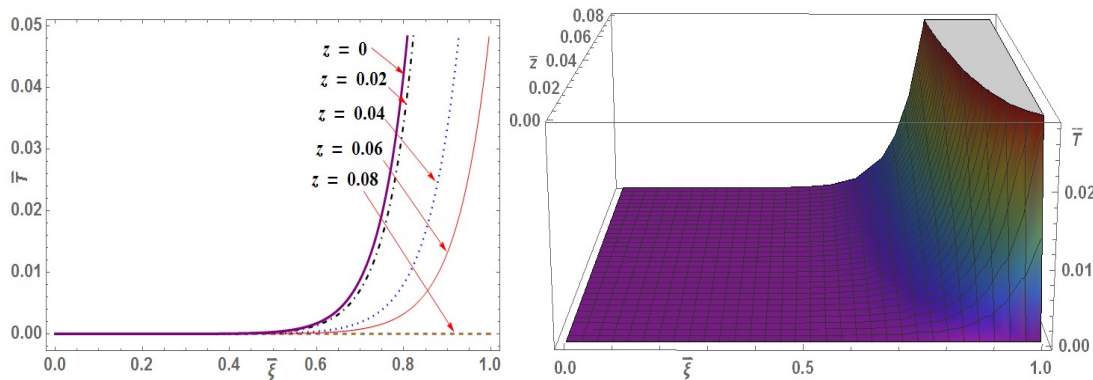


Fig. 2. Temperature distribution along ξ for different values of z .

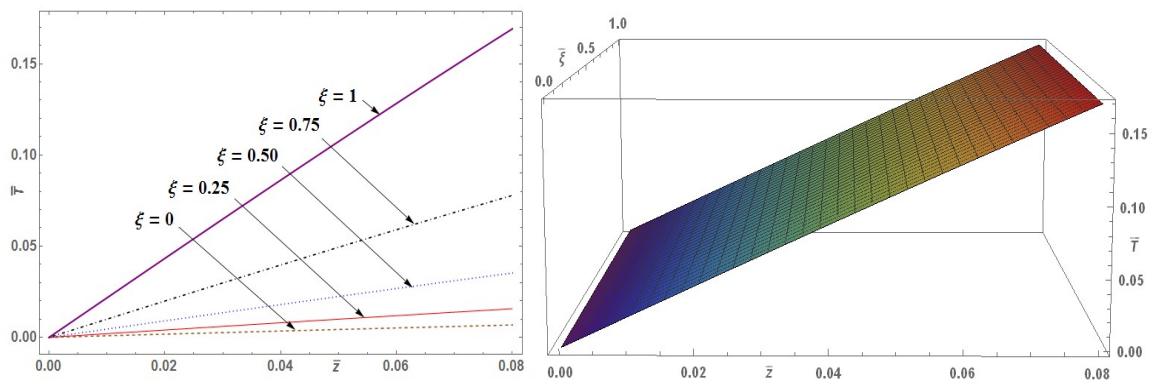


Fig. 3. Temperature distribution along z for different values of ξ .

As shown in Fig. 2, the temperature increases along the radial direction and reaches a maximum at the outer part. The maximum values of the temperature magnitude arise due to additional heat supply. The distribution of the temperature gradient at each instance decreases at the axial direction and procures minimum at the lower face which is kept at zero temperature. It is observed in Fig. 3 that the expansion occurs on the outer edge due to the sectional heat supply followed by the compressive

stress occurring at the inner core of the ellipse.

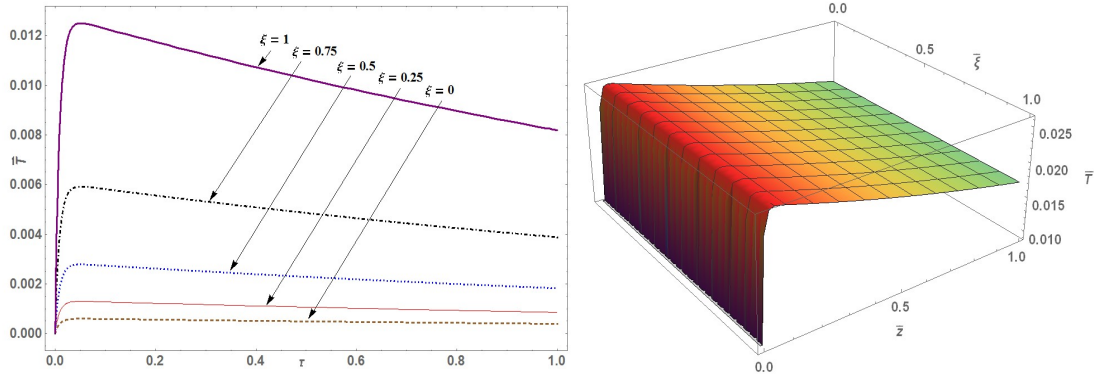


Fig. 4. Temperature distribution along τ for different values of ξ .

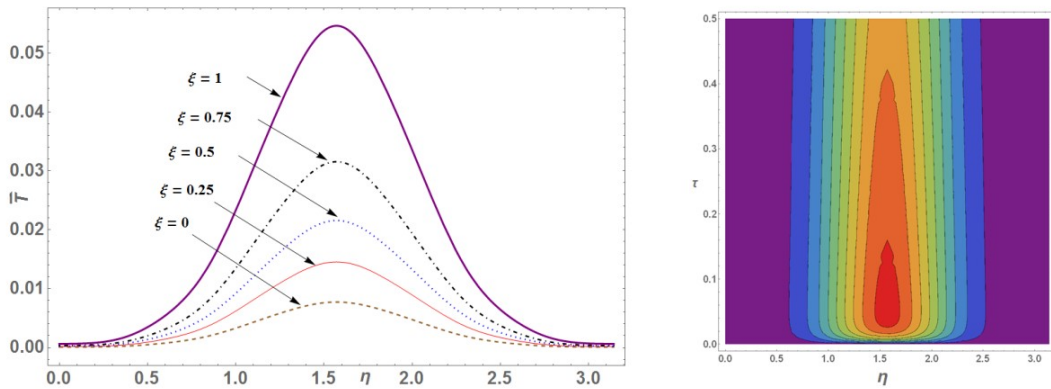


Fig. 5. Temperature distribution along η for different values of ξ .

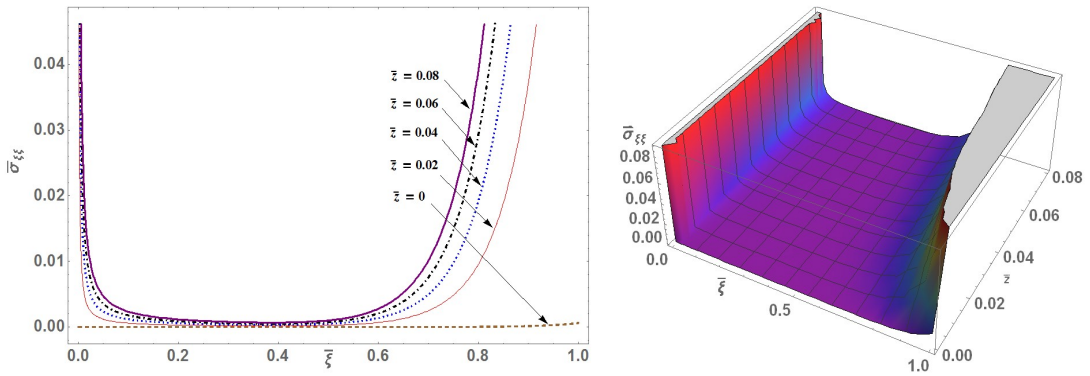


Fig. 6. Radial stress distribution along ξ for different values of z .

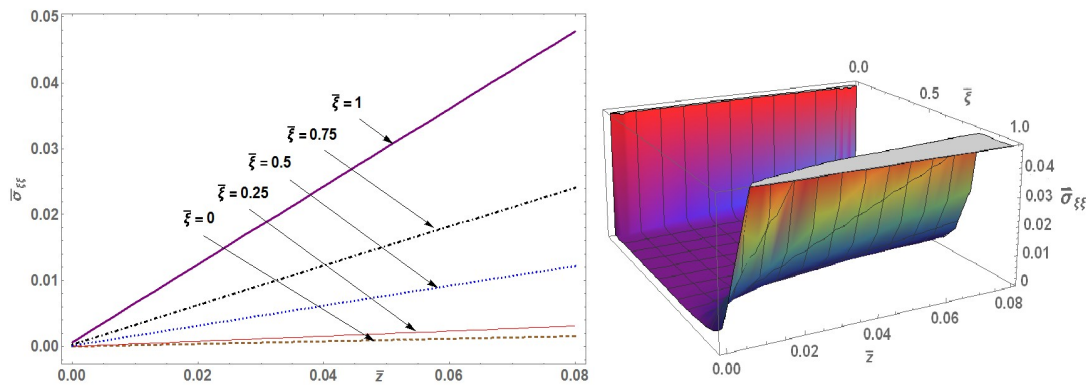


Fig. 7. Radial stress distribution along z for different values of ξ .

As can be seen, Fig. 4 indicates the time variation of temperature distribution along the axial direction of the plate. The maximum value of the temperature magnitude occurs at the outer edge due to the supplemental heat supply on the body. The distribution of the dimensionless temperature gradient at each time point decreases towards the unheated area of the central part of the ellipse boundary inclining below zero in one direction. The temperature profile along the angular direction is illustrated in Fig. 5 where the temperature trend reaches the maximum along the angular direction at the mid-core for a fixed value of $\bar{\xi}$. On the other hand, at the central part of the thickness, the temperature fluctuation becomes stable due to the accumulation of energy as a result of more exposure to heat sources, therefore, the thermal expansion is more at the central part of the plate which leads to a high tensile force.

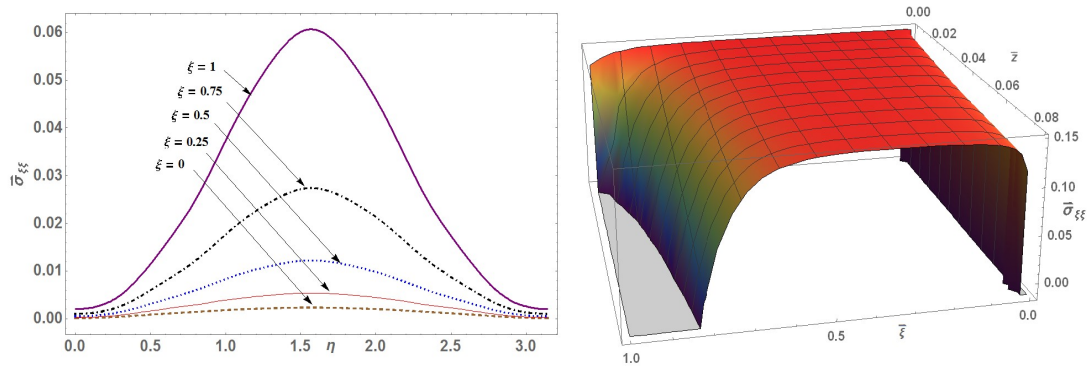


Fig. 8. Radial stress distribution along η for different values of ξ .

The dimensionless thermal stresses along the radial direction having minimum tensile stress at the central part while more tensile stress occurring at the outer part of the plate are illustrated in Fig. 6. The radial stresses distribution along the axial direction of the plate is shown in Fig. 7. The maximum value of the stress magnitude occurs towards the outer edge due to the supplemental heat supply. The maximum tensile stress at the mid-core, and the compressive stress occurring at the outer part of the plate are shown in Fig. 8. Its absolute value increases with time due to the accumulation of thermal energy dissipated by the sectional and internal heat supply.

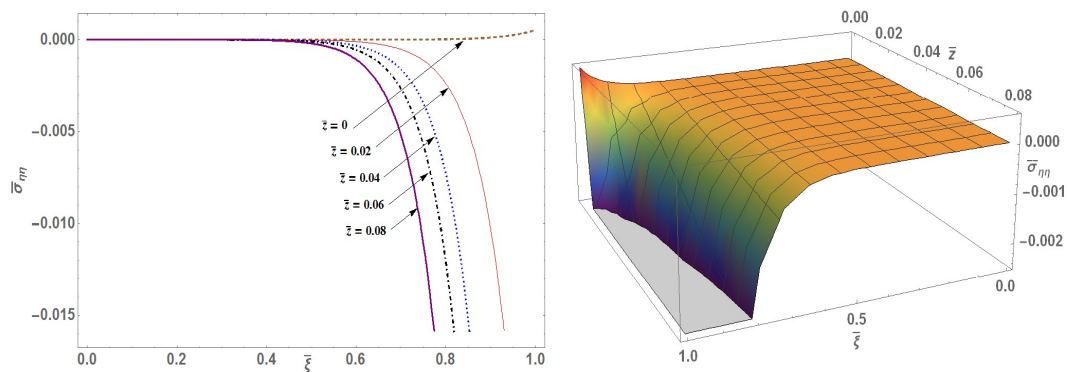


Fig. 9. Tangential stresses distribution along ξ for different values of z .

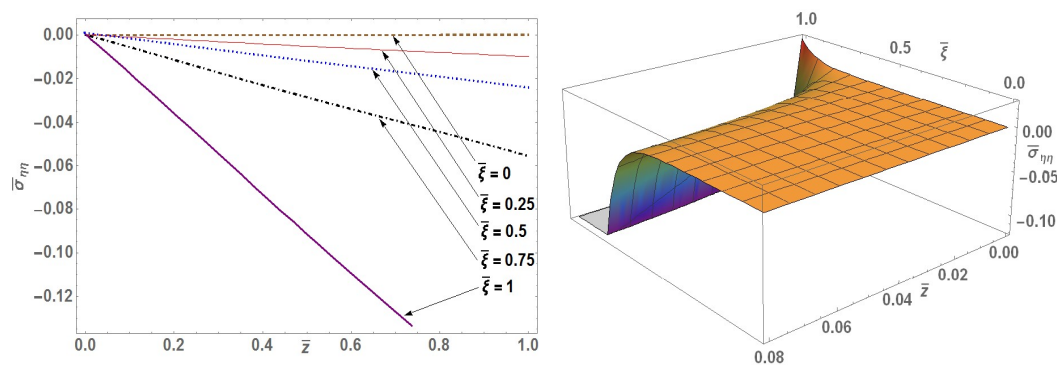


Fig. 10. Tangential stresses distribution along z for different values of ξ .

The dimensionless normal stress $\bar{\sigma}_{\eta\eta}$ along the radial direction with the maximum stress value occurring at the inner edge $\bar{\xi} = 0$ is illustrated in Fig. 8 that is energized due to the sectional heat supply. On the other hand, Fig. 10 depicts that the tangential stress $\bar{\sigma}_{\eta\eta}$ attains the maximum expansion at the inner part due to the accumulation of thermal energy dissipated

by the sectional heat supply. As can be seen, Fig. 11 shows the minimum tensile stress at the center, and the compressive stress at both terminuses of the plate where its absolute value increases with time.

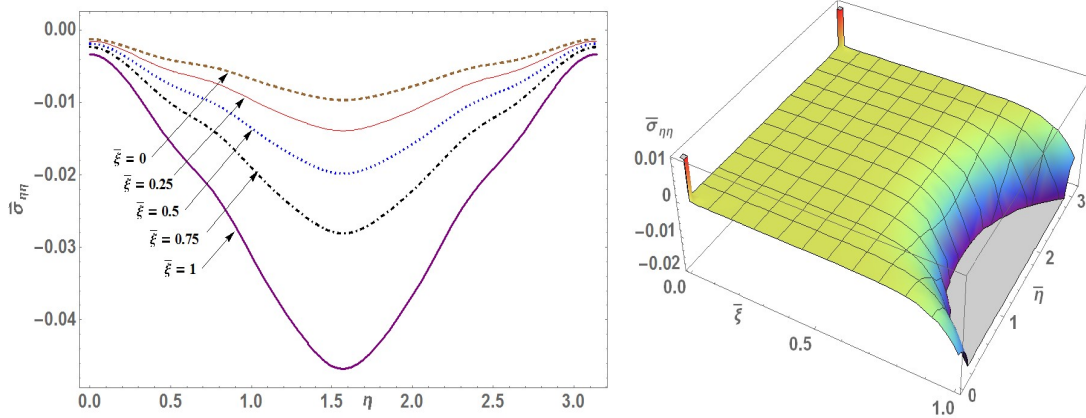


Fig. 11. Tangential stresses distribution along η for different values of ξ .

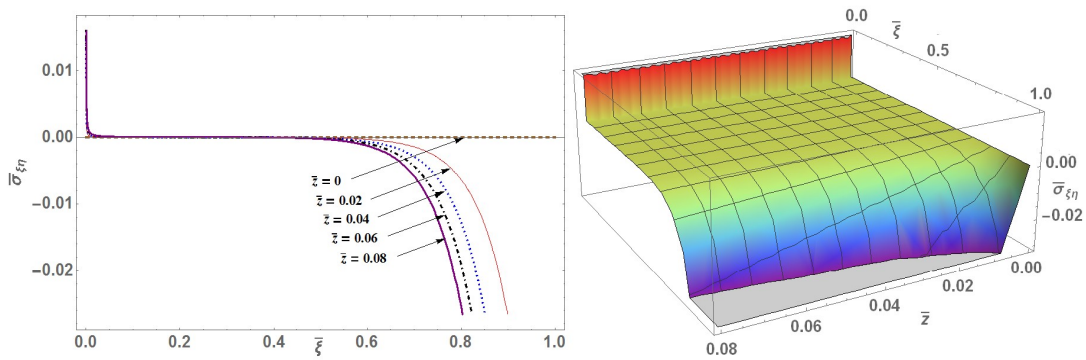


Fig. 12. Shear stresses distribution along ξ for different values of z .

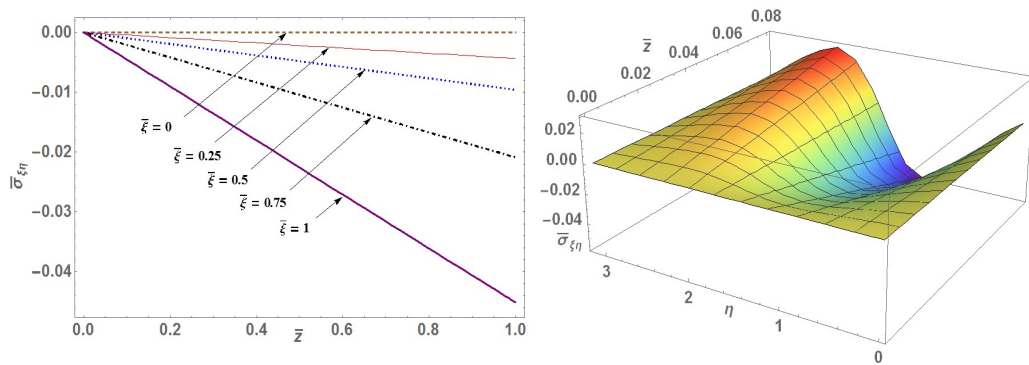


Fig. 13. Shear stresses distribution along z for different values of ξ .

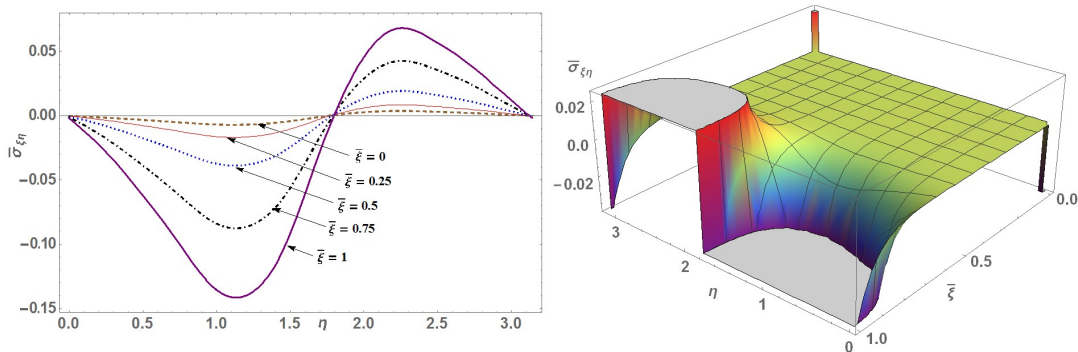


Fig. 14. Shear stresses distribution along η for different values of ξ .

The expansion occurs on the outer edge due to the sectional heat supply followed by the compressive stress occurring on the inner core of the ellipse (Figs. 12). The absolute value tends to be zero as it proceeds towards the shear stress profile.

Moreover, Fig. 13 depicts that the stress $\bar{\sigma}_{\xi\eta}$ procures the maximum expansion at the inner part due to the accumulation of thermal energy dissipated by the sectional heat supply. The distribution of shearing stress $\bar{\sigma}_{\xi\eta}$ along the \bar{z} -direction on $\bar{\xi} = 1$ is shown in Fig. 14 where it attains the sinusoidal due to the accumulation of thermal energy dissipated by the sectional heat supply, and its absolute value increases with time. The values after $\bar{\xi} \geq 0.25$ are nearly zero along the \bar{z} -direction.

5. Transition to circular plate

When the elliptical plate tends to a circular plate of radius a , the semi-focal $c \rightarrow 0$, therefore, λ_n is the root of the transcendental equation $J_0(\alpha_n) = 0$. Moreover, $e \rightarrow 0$ as $\xi \rightarrow \infty$, $\sinh(\xi) \rightarrow \cosh(\xi)$, $h \cosh(\xi) \rightarrow r$ [as $h \rightarrow 0$], $\cosh(\xi)d\xi \rightarrow r dr$, $\cosh(2\xi)d\xi \rightarrow 2 \cosh(2\xi)\sinh(2\xi)d\xi \rightarrow 2rdr / \ell^2$, $h \sinh(\xi)d\xi \rightarrow dr$. Using results from [15],

$$\begin{aligned}
 Ce_0(\xi, q_{n,0}) &\rightarrow p'_0 J_0(\lambda_n r), \quad Ce'_0(\xi, q_{n,0}) \rightarrow p'_0 J'_0(\lambda_n r), \quad Ce''_0(\xi, q_{n,0}) \rightarrow p'_0 J''_0(\lambda_n r), \quad ce_0(\eta, q_{n,0}) \rightarrow 1/\sqrt{2}, \\
 A_0^{(0)} &\rightarrow 1/\sqrt{2}, \quad A_2^{(0)} \rightarrow 0, \quad \Theta_{2n,0} \rightarrow 0, \quad \lambda_{n,0}^2 = \alpha_n^2 / a^2 = \lambda_n^2, \quad p'_0 = Ce_0(0, q_{n,0}) ce_0(2\pi, q_{n,0}) / A_0^{(0)}
 \end{aligned}
 \tag{32}$$

Then, Eq. (21) is degenerated into

$$T(r, z, t) = \sum_{\ell=1}^{\infty} \sum_{n=0}^{\infty} \bar{T}(\lambda_n, \ell, t) \sin(\alpha_m z) p'_0 J_0(\alpha_0 a_0 / a) / \sqrt{2} C_n
 \tag{33}$$

in which

$$\bar{T}(q_n, m, t) = \exp[-(\kappa \lambda_n^2 / a^2 + \alpha_m^2) t] \left\{ \int_0^t \exp[(\kappa \lambda_n^2 / a^2 + \alpha_m^2) \tau] \alpha_m \bar{f} d\tau \right\},
 \tag{34}$$

$$\bar{f} = Q_0 \exp(-\omega t) [\cosh(2a) - 1] p'_0 J_0(\lambda_0 a_0) / \sqrt{2}
 \tag{35}$$

and

$$C_n = \bar{f}(q_n) \left\{ \int_0^a r [p'_0 J_0(\lambda_0 r)]^2 dr \right\} / 2\pi
 \tag{36}$$

The above-mentioned results are in a good agreement with the previously studied results [16].

6. Conclusion

The proposed analytical solution of the transient thermal stress problem of the confocal elliptical region was handled in the elliptical coordinate system. To the author’s cognizance, there have been no reports of the solution so far in which the elliptical plate of the finite height with Dirichlet type boundary conditions and the prescribed surface temperature on the curved surface is considered. The analysis of transient three-dimensional equation of heat conduction was conducted using the integral transformation method, and the thermal bending stresses were obtained utilizing the transverse displacement function. The following results were obtained during the research:

- The advantage of this method was its generality and its mathematical power to handle variants of thermo-mechanical boundary conditions.
- The maximum tensile stress shifting from central core to outer region might be due to heat, stress, and concentration under considered temperature field.
- The value of shearing stress became profoundly and immensely colossal near the inner edge and comparatively more minute at the outer edge.
- Finally, the maximum tensile stress occurred at the circular core on the major axis compared to the elliptical central part designating the distribution of impuissant heating. It might be due to inadequate perforation of heat through the elliptical inner surface.

Nomenclature

x, y, z	rectangular Cartesian coordinates	κ	thermal diffusivity
ξ, η, z	elliptic-cylindrical coordinates	q_n, m	parametric roots of the transcendental equation
ℓ	thickness of the plate	$f(\xi, \eta, t)$	heat supply available on the curved surface
W	deflection normal to the plate	$2c$	focal length = $2(a^2 - b^2)^{1/2}$
D	flexural stiffness of the plate [$D = E \lambda^3 / 12(1 - \nu^2)$]	ξ_0	= $\tanh^{-1}(b / a)$
q	parameter of Mathieu equation	∇^2	Laplacian operator
$ce_n(\eta, q)$	ordinary Mathieu function of the first kind of order n	E	Young’s modulus

$Ce_n(\xi, q)$	modified Mathieu function of the second kind of order n	ν	Poisson's ratio
h	scale factor	α	coefficient of thermal expansion

References

- [1] K. C. Jane, C. C. Hong, Thermal bending analysis of laminated orthotropic plates by the generalized differential quadrature method, *Mechanics Research Communications*, 27(2), 2000, 157-164.
- [2] M. E. Mathews, M. S. Shabna, Thermal-static structural analysis of isotropic rectangular plates, *IOSR Journal of Mechanical and Civil Engineering*, 11(5), 2014, 36-45.
- [3] K. C. Deshmukh, M. V. Khandait, R. Kumar, Thermal stresses in a simply supported plate with thermal bending moments with heat sources, *Materials Physics and Mechanics*, 21, 2014, 135-146.
- [4] X. Cheng, J. Fan, Thermal bending of Rectangular Thin Plate with two opposite edges clamped, one edge simply supported and one edge free, *KSCE Journal of Civil Engineering-Seoul*, 20(1), 2016, 333-342.
- [5] I. A. Okumura, Y. Honda, J. Yoshimura, An analysis for thermal-bending stresses in an annular sector by the theory of moderately thick plates, *Structural Engineering*, 6(2), 1989, 347-356.
- [6] Z. Dong, W. Peng, J. Li, F. Li, Thermal bending of circular plates for non-axisymmetrical problems, *World Journal of Mechanics*, 1(2), 2011, 44-49.
- [7] E. Ventsel, T. Krauthammer, *Thin plates and shells theory, analysis and applications*, Marker Dekker., New York (2001).
- [8] P. A. A. Laura, C. Rossit, Thermal bending of thin, anisotropic, clamped elliptic plates, *Ocean Engineering*, 26(5), 1998, 485-488.
- [9] K. Sato, Bending of a simply-supported elliptical plate under the combined action of uniform lateral load and in-plane force, *Theoretical and Applied Mechanics-Japan*, 54, 2005, 31-44.
- [10] P. Bhad, V. Varghese, L. Khalsa, Thermoelastic theories on elliptical profile objects: An overview and perspective, *International Journal of Advances in Applied Mathematics and Mechanics*, 4(2), 2016, 12-60.
- [11] P. Bhad, V. Varghese, L. Khalsa, Heat source problem of thermoelasticity in an elliptic plate with thermal bending moments, *Journal of Thermal Stresses*, 40(1), 2016, 96-107.
- [12] P. Bhad, V. Varghese, L. Khalsa, Thermoelastic-induced vibrations on an elliptical disk with internal heat sources, *Journal of Thermal Stresses*, 40(4), 2016, 502-516.
- [13] T. Dhakate, V. Varghese, L. Khalsa, Integral transform approach for solving dynamic thermal vibrations in the elliptical disk, *Journal of Thermal Stresses*, 40(9), 2017, 1093-1110.
- [14] R. K. Gupta, A finite transform involving Mathieu functions and its application, *Proceedings of the National Academy of Sciences, India Section A*, 30(6), 1964, 779-795.
- [15] N. W. McLachlan, *Theory and Application of Mathieu function*, Oxford Univ. Press, Pp. 21, 27, 159, 175-176, 1947.
- [16] V. Varghese and N. W. Khobragade, Alternative solution of transient heat conduction in a circular plate with radiation, *International Journal of Applied Mathematics*, 20(8), 2007, 1133-1140.